Analysis of implant breakage in trochanteric fractures

C. DEMIAN*, V.-A. ŞERBAN, A. RĂDUȚĂ, I. VIDA-SIMITI[a], R. PREJBEANU[b], C. LOCOVEI
"Politehnica" University of Timişoara, Faculty of Mechanics
[a]The Techincal University of Cluj-Napoca, the Faculty of Materials Science and Engineering
[b]"Victor Babes" University of Medicine and Pharmacy, Timisoara

The paper analysis the failure mechanism by breakage of a stainless steel AISI 316Ti plate, currently used for trochanteric fractures. The plate was removed from the body of a patient and then was subjected to tests. The implant was analyzed by optical and electronical microscopy and reveals a higher content of inclusions that lead to a severe form of corrosion in the area of screws for fastening, but also on free surfaces. The results obtained through finite elements analysis reveal that the frictional stresses and slipping tendencies at the interface implant- superior part of femur reach a maximum value in areas where fracture has occurred.

(Received May 15, 2009; accepted May 26, 2009)

Keywords: Implant, Trochanteric fracture, Crack, Nonmetallic inclusions, Fatigue facture

1. Introduction

Recovering and analysing the implants offer critical informations that lead to a better understanding of phenomenae on the implant-bone interface. Direct bone-metal osteointegration of the implants, in the form of stainless steel rod, was possible only due to the carefully controlled surgical techniques and the careful preparation of the surface of the implants [1], [2]. In order to facilitate the bone growth, porous layers over implants can be applied; relation between the sizes of pores and bone growth were obtained by studying recovered implants [3].

Some of the models of the osteosynthesis plates, used for different fractures, reveal significant corrosion, attributed initially to the use of a combination of metals (for example: AISI 316L fixed with AISI 304L screws) and later both to micro-galvanic corrosions and corrosion through micro-movements and friction between the components [4], [5], [6], [7].

2. Material and Methods

The mechanism of corrosion was studied on a recovered failure implant used for osteosynthesis of trochanteric fractures as 130° Angled Blade Plate, (DCP), made from austenitic stainless steel (Fig. 1).

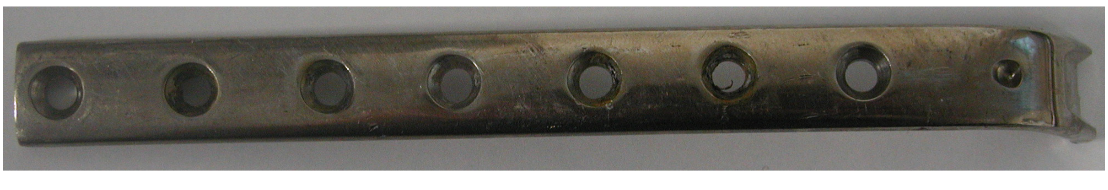

Fig. 1. Osteosynthesis plate for trochanteric fractures

Chemical composition of implant material was determined with optical emission spectrometer (*ARL QuantoDesk Spectrometer).*

Implant was metallographically prepared in a transversal sections, with the purpose of examination through optic metallographic microscope *Olympus BX51M.*

Before extracting the sample and microscopic investigation, aspect of corroded surfaces was investigated by a *stereo Olympus SZX7* microscope.

As a means to quantify the maximum tolerable levels of stresses and strains of the implant-bone assembly a finite element analysis was carried out. The implant-bone assembly was subjected to loads and constraints similar to those found in human body. The mechanism of fatigue fracture was analyzed using the AFGROW program.

3. Results

3.1 Examination of fractured angled blade plate through optic and electronic microscope

Table 1 shows experimentally determined chemical composition for angled blade plate, while table 2 shows equivalent chemical composition corresponding to ASTM standards (AISI 316Ti).

Table 1. Composition of analysed implant material.

Element	*Concentration (%)*	*Element*	*Concentration (%)*
Fe	68.20	Ni	10.01
C	0.0435	Mo	2.428
Si	0.3622	Cu	0.1865
Mn	1.476	Ti	0.3591
P	>0.046	Nb	<0.003
S	0.0104	Co	0.1358
Cr	16.64		

Chemical composition of tested alloy falls in the category of Stainless steel AISI 316Ti, according to ASTM A 240-00.

The fracture surface presents the aspect of a fatigue fracture, while the crack propagation was present in two zones (Fig. 2 a, b and c).

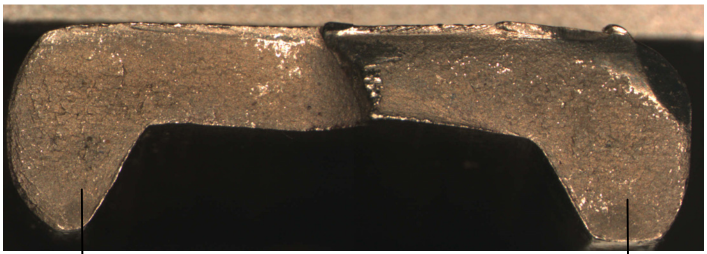

a) OM 10x

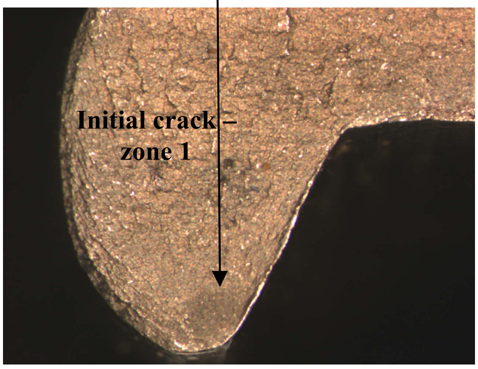

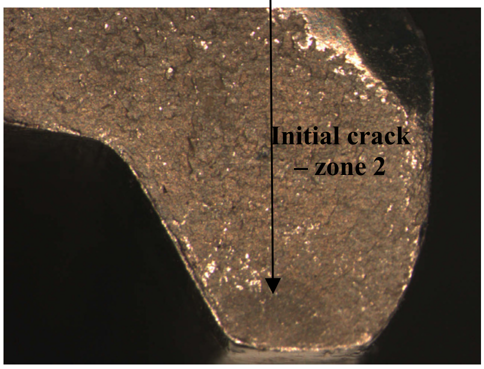

b) OM 16x *c) OM 16x*

Fig. 2. The aspect of blade plate surface fracture

Microstructures of the tested sample from different areas, after the metallographic preparation and chemical etching (Fig. 3) confirm the existence of some orientated series of nonmetallic inclusions, due to the plastic deformation.

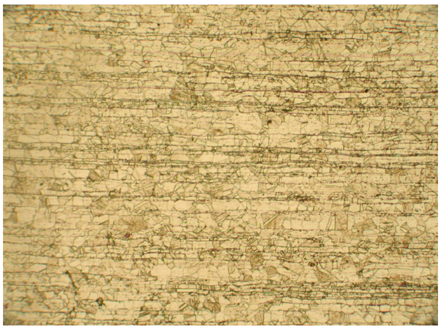

a) OM 100x

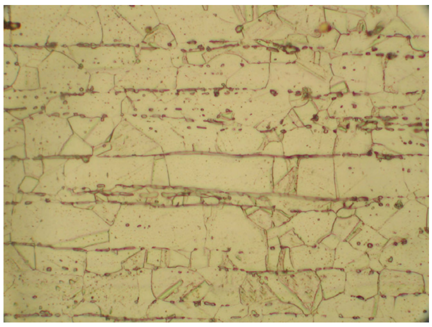

b) OM 500x

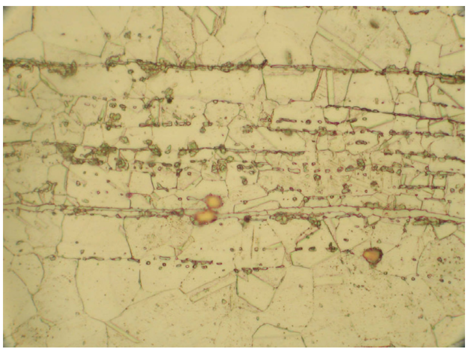

c) OM 500x

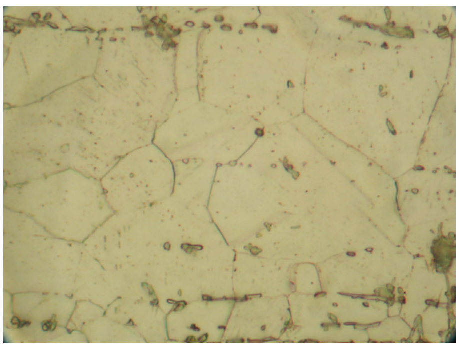

d) OM 1000x

Fig. 3. Microstructures corresponding to plate used in osteosynthesis of trochanteric fractures implants

The examined material has a high content of inclusions as titanium nitrides, carbonitrides and chemical compounds as silicates, which lead to a severe form of corrosion in the area of screws for fastening, but also on free surfaces. It is presumed that cyclic loads, favored by corrosion (fatigue corrosion) have produced the fracture.

3.2 The finite elements analysis

The finite element analysis was performed using ANSYS 10 software. A femoral model formed of cortical and spongy bone structure, filled with marrow was taken in consideration [7], [8]. The material properties (ASISI 316Ti stainless steel) of fracture implant and the properties of the cortical and spongy bones and the marrow are presented in the Table 2.

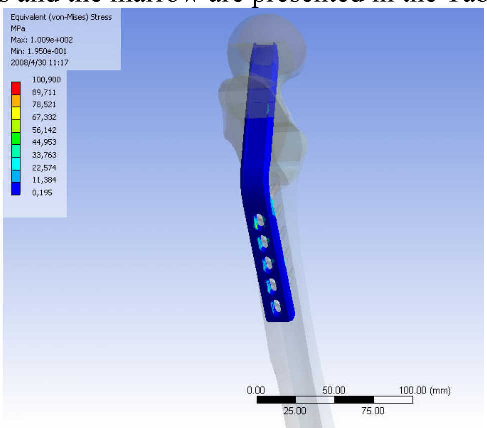

Fig. 5. The equivalent stresses from implant, in the case of reduce friction between the fractured bones

Table 2. The mechanical and physical properties considered in the FEM analyses .

No.	***Properties***	***Value***			
		AISI 316Ti stainless steel	*Cortical bone*	*Spongy bone*	*Marrow*
1	Young modulus	$1{,}96\times10^{11}$ Pa	$1{,}37\times10^{10}$ Pa	3.89×10^{8} Pa	$1{,}1\times10^{9}$ Pa
2	Poisson ratio	0,39	0.3	0.28	0.42
3	Density	7900 kg/m³	1,7 g/cm³	500 kg/m³	950 kg/m³
4	Yield tensile strength	2.00×10^{8} Pa	$1{,}2\times10^{8}$ Pa	7.36×10^{6} Pa	$2{,}5\times10^{7}$ Pa
5	Tensile strength	5.50×10^{8} Pa	$0{,}9\times10^{8}$ Pa		

The finite element analysis were made using the following assumptions: the weight of the patient is 80 Kg (G); during ***walking*** the value of the resultant force (R) is 3100 N, calculated by equation $R = (4...4{,}5)\cdot G$, the components of resultant force are $R_x = -1060{,}13$ N; $R_y = 0$; $R_z = 2913{,}1$ N.

The discreet element mesh, having 25785 nodes and 14857 elements is presented in Fig. 4 a. Figure 4 b presents the model with highest loads applied, the connection between components being of bounded type, which means that nodes stay in contact during the deformation of the model subjected to loads [9].

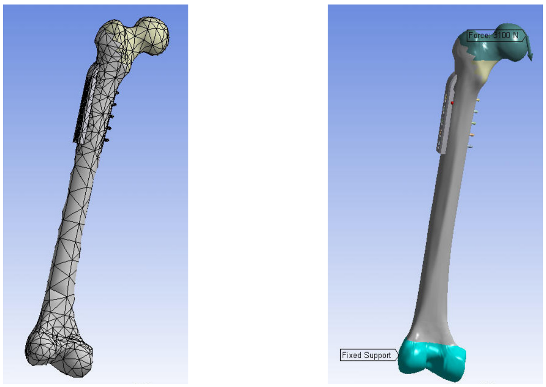

a) mashed model *b) force applied on structure*

Fig. 4. Presentation of initial data for finite elements analysis

The Von Mises stresses, that appear in the fixed implant in the case of reduce friction between the fractured bones are presented in Figure 5. This means there is a possibility of relative motion into the contact zone and represents the initial case, when the fractured bones were not fitted by callus increase. The fractured bones were fitted merely by implant.

The Von Mises stresses that appear in the fixed implant in the case of the fractured bones are beginning to fit by callus are presented in the Figure 6. The contact from the fracture zone is “no separation” type. This mean that the contact permits micromotions between the finite elements nods in the contact zone, without a relative motion of the fractured parts bone.

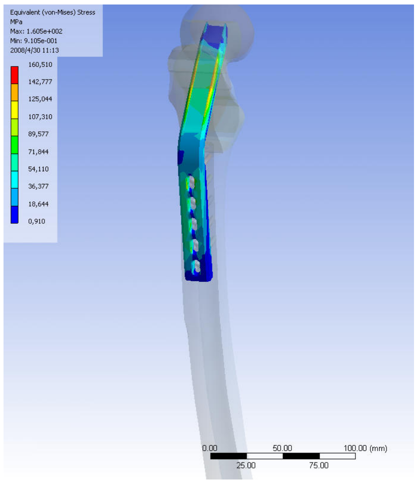

Fig. 6. The equivalent stresses from implant, in the case of the fractured bones fitted by callus

The stresses from implant decrease as the friction between the fractured parts increase. The maximum load values are positioned near the fatigue fractured zone.

3.3 The fatigue fracture analyses

The damage of the angled blade plate is due to the cyclic loads that were amplified by the action of corrosion (fatigue corrosion). These lead to brakeage and require the analyses of the fatigue fracture.

Fracture analyses of the recovered angled blade plate were realized using NASGRO equation numerically solved using AFGROW software. The recovered angled blade plate fracture is due to material fatigue. The goal of the fracture analysis is the numerical calculus of the cycles or of the number of steps made by the patient, until the plate fractures. The level of stresses used in NASGRO equation were the ones previously calculated by means of finite element analysis [10]. The method used by AFGROW is closed form solution, in this particular case, classic model of single edge corner crack has been used. Two identical semielliptical initial cracks were taken into consideration in order to calculate the number of cycles that lead to the fracture. The analysis were performed using initial crack depth, *a*, equals to 0.1 mm and initial crack length, *c*, equals to 1 mm. Such cracks can be easily produced by scratching during the implantation process and are enlarged by the natural corrosion due to the body fluids.

For a given material the crack growth rate, *da/dN*, is a complex function of many variables including stress intensity range ($\Delta K = K_{max} - K_{min}$), stress ratio ($R = K_{min} / K_{max}$), temperature and frequency of the applied cyclic load. In the most general form it is simply written as:

$$\frac{da}{dN} = f(\Delta K, R, T, f, ...) \tag{1}$$

Where:

da/dN – crack depth growth rate;

ΔK – stress intensity factor range ($\Delta K = K_{max} - K_{min}$);

A number of explicit equation forms exist to cater for simplified situations e.g. the Paris (equation 2) and Walker (equation 3).

$$\frac{da}{dN} = C \cdot (\Delta K)^n \tag{2}$$

$$\frac{da}{dN} = C_0 \left[\Delta K (1 - R)^{m-1}\right]^n \tag{3}$$

Where:

C, n – fit parameters in the NASGRO equation;

m – shape parameter of the Weibull distribution of the fracture resistance.

For the most general approach, the evaluation of *da/dN* must allow input of as many of the contributing factors as possible. An advanced approach is the so-called NASGRO expression (also called Forman–Newman–de Koning equation) jointly introduced by *National Aeronautics and Space Administration* (NASA) and *European Space Agency* (ESA), which is now common in aerospace applications [10], [11], [12]:

$$\frac{da}{dN} = C \cdot (\Delta K_{eff})^n \cdot \frac{\left[1 - \frac{\Delta K_0}{\Delta K_{eff}}\right]^p}{\left[1 - \frac{K_{max}}{K_{Jc}}\right]^q} \tag{4}$$

Where:

ΔK_{eff} – effective stress intensity factor range ($\Delta K_{eff} = K_{max} - K_{op}$, K_{op} – opening stress intensity factor, above which the crack is open);

ΔK_0 – threshold stress intensity factor range;

K_{Jc} – fracture resistance of the material written in the terms of *K*;

p, q – fit parameters in the NASGRO equation.

The fatigue fracture analysis was completed using the following geometrical conditions and material properties: crack depth *a*= 0.1 mm, crack length *c* = 1 mm, plate thickness T = 2 mm, plate width W = 10 mm and material properties were those for the wrought AISI 316Ti as in Table 3.

Table 3. Mechanical and physical properties of the material

Material properties	*AISI 316Ti*
Coefficient of Thermal Expansion	$1{,}26 \times 10^{-5}$
Effective fracture toughness for surface/elliptically shaped crack, KV at the 37 °C, J	153,838
Yield stress, $R_{p0,2}$, MPa	689,476
Paris crack growth rate constant	$7{,}6575 \times 10^{-12}$
Plane stress/strain constraint factor	2,5

The propagation curves *a* and *c* versus number of cycles are presented in the figure 7.

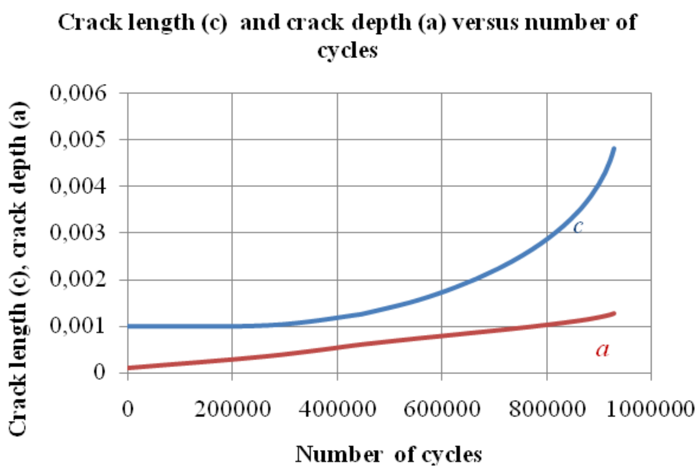

Fig. 7. The evolution of the cracks propagation versus number of cycles

The angled blade plate fractures after approximately 1.000.000 cycles that explain the fact that the plate life span is about 1 year assuming daily load of the plate cumulate with material defects and surface scratches or microcracks.

4. Conclusion

The aspect of fracture surface and microstructure of the material reveals the presence of some material defects (non metallic inclusions) that increases the probability of fatigue fracture of the implant and lead to a higher rate of material corrosion.

The values obtained after simulation confirms this hypothesis. The maximum value of calculated stress is 160.5 MPa and does not reach the level 200-250 MPa that corresponding to yield tensile strength of AISI 316Ti stainless steel.

Acknowledgements

All the investigations were performed in the Research Center for the Processing and Characterisation of the Advanced Materials of the "Politehnica" University of Timisoara.

The research was performed in the framework of COST ACTION 537 Core Laboratories for the Improvement of Medical devices in Clinical Practice from the Failure of the Explanted Prostheses Analysis (FEPA).

References

[1] T. Albrektsson, P. I.Branemark, H. A. Hansson, Lindstrom J. Acta Orthop. Scand., **52,** 155-170 (1982).
[2] D. Drăgulescu, C. Demian, I.Vida Simiti, A. Răduță, R. Prejbeanu, International Conference on Biomaterials & Medical Devices, BiomMed'2006, Conference proceeding, Abstract Volume, November, 9-11th, 2006, Iasi, Romania, ISBN 973-718-566-8; 987-973-718-566-2, p. 176.
[3] S. D.Cook, R. L. Barrack, K. A. Thomas, R. J. Haddad Jr., Quantitative analysis of tissue growth into human porous total hip components, J. Arthroplasty, **3,** 249-262, (1988)
[4] Collier J.P., Suprenant V.A., Jensen R.E., Mayor M.B., Clin. Orthop., **271**, 305-312 (1991).
[5] Mathiasen E.B., Lindgren J.U., Biomgren G.G.A., Reinholt F.P., J. Bone Joint Surg., **73B**: 569-575 (1991).
[6] Brown S.A., Flemming C.A.C., Kawalec J.S., Placko H.E., Vassaux C., Merritt C., Payer J.H., Kraay M.J., J. Appl. Biomater., **6**, 19-26 (1995).
[7] Drăgulescu D., Demian C., Rusu L., Răduță A., Popescu M., Cucuruz L. R., Prejbeanu R., Vida Simiti I., Properties and Behavior of an Orthopedic Implant, Materialprufung (MP Materials Testing), ISSN: 0025-5300, 05, Page 250-255, 2008
[8] Sudhakar, K.V., Metallurgical investigation of a failure in 316L stainless steel orthopedic implant. In: Engineering Failure Analysis, **12**, 249–256 (2005).
[9] Lemons, J.E., Lucas L.C.: Properties of biomaterials. J. Arthroplasty, 1(2): 143–7, 1986
[10] Demian C., Researches regarding the behavior of osseous implantation materials according to quality European standards, Edited by Politehnica, Timisoara, 2007
[11] NASGRO, Fatigue Crack Growth Computer Program, NASGRO, version 3, NASA, L.B. Johnson Space Centre, Houston, Texas. JSC-22267B, 2000
[12] Raduta A., Nicoara M., Locovei C., The Influence of Residual Stresses on the Fatigue Resistance of Axles Used in the Construction of Railway Equipment, International Conference on CRACK PATHS (CP 2006), Parma (Italy), 14th - 16th September, University of Parma-Via Università, 12, European Structural Integrity Society, 2006

*Corresponding author: camelia.demian@mec.upt.ro